

Ultraviolet elimination of H₂ from chloroethylenes

Guoxin He, Yuangan Yang,^{a)} Yibo Huang, Satoshi Hashimoto,^{b)} and Robert J. Gordon
Department of Chemistry (m/c 111), University of Illinois at Chicago, Chicago, Illinois 60607-7061

(Received 21 April 1995; accepted 27 June 1995)

The elimination of H₂ in the photodissociation of mono- and di-chloroethylenes was studied with a pump-and-probe technique. A 193 nm excimer laser was used to photodissociate the parent molecules, and a tunable dye laser was used to probe the H₂ fragment by 2+1 resonance-enhanced multiphoton ionization (REMPI). The nascent rotational state distributions of H₂(X¹Σ_g⁺, v''=0–4) were extracted from the REMPI spectra, and were found to have Boltzmann-type distributions. The maximum and average translational energies for some of the rovibrational levels of H₂ were measured using magic angle Doppler spectroscopy. The translational energy of the fragments plus the internal energy of H₂ was found to exceed the available energy for a three-center elimination mechanism. It is concluded that a migration mechanism plays a significant role in H₂ elimination. © 1995 American Institute of Physics.

I. INTRODUCTION

Chloroethylene molecules are prototypical cases for studying the photodissociation dynamics of substituted olefins.¹ The photochemistry of these molecules has been investigated for many years, and a brief history of this subject is presented in the previous paper (hereafter referred to as paper I).² The very large oscillator strengths of these molecules near 193 nm correspond to a π→π* excitation of the double bond.³ Molecules excited by this transition do not react directly, but rather undergo nonadiabatic transitions either to other excited states or to the ground state. The primary dissociation products are Cl, HCl, H, and H₂ (and their organic partners, listed in order of relative yields). The branching fractions for the dichloroethylene (DCE) isomers are given in Table I.

This paper is part of a continuing study of the photodissociation dynamics of vinyl chloride (VCl) and DCE. Previous papers dealt with the state distributions of the Cl, H, and HCl fragments.^{1,2,4,5} A summary of these results is helpful for comparison with the dynamics of H₂ elimination, which is the subject of the present study. The Cl atom is produced both on an excited potential energy surface (PES) and on the ground surface. For VCl, ~80% of the Cl atoms are produced on the excited PES, while for DCE this fraction drops to 40%–45%.² Reaction on the excited surface is prompt, producing anisotropically recoiling fragments with nonstatistical distributions of kinetic energy. In contrast, the ground surface reaction gives isotropic, statistical products.

The other photofragments are produced exclusively on the ground PES. The hydrogen atom reaction is a simple bond rupture on the ground PES. The most striking feature of the HCl channel is that the rotational populations for HCl(v''=0) and HCl(v''=1 and 2) are qualitatively different. For v''=0, bimodal distributions were observed for five parent molecules (VCl, CH₂CDCl, and the three DCE isomers),

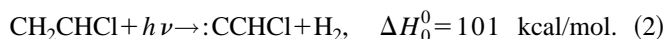
while for v''>0 linear Boltzmann plots were always observed. Similar results were reported by Sato *et al.* for DCE.⁶ The similarity of the rotational distributions for these molecules suggests a common mechanism. A dichotomy between HCl(v''=0) and HCl(v''>0) was also observed in the translational energy distributions of HCl/VCl. (Here and throughout the paper HCl/VCl refers to the HCl fragment produced by photodissociating VCl, with corresponding notation for other parents and fragments.) The former showed a positive correlation between the 1D average translational energies and the rotational angular momentum, while for v''>0 there was no correlation.

Another notable aspect of the HCl channel are the relative quantum yields of HCl for different parent molecules. The HCl/VCl yield is four times that of HCl/CH₂CDCl,⁴ indicating a preference for three center elimination (3CE) to produce vinylidene. Measurements of the translational energy distribution of HCl indicated, however, that the recoil energy is greater than expected for a simple 3CE mechanism. To reconcile these observations we proposed a mechanism in which α,α elimination of HCl and isomerization of vinylidene to form acetylene occur in a concerted, nonsynchronous fashion, so that some of the energy released by the isomerization step is transferred to the recoiling fragments.²

The only previous report of the H₂ fragment is that of Ausloos *et al.*,⁷ who excited partially deuterated VCl(CH₂CDCl, *d*-VCl) at 147 nm in the presence of radical scavengers and detected the organic fragments with a gas chromatograph. The reported quantum yields are 5% for H₂ and 1% for HD. Many of the issues involved in HCl elimination—the nature of the product state distributions, three center vs four center mechanisms, the role of atom migration, the effects of exit channel barriers—apply also to H₂. The reaction enthalpies for H₂/VCl are^{8,9}



and



^{a)}Permanent address: DOTY Scientific, Inc., 700 Clemson Rd., Columbia, South Carolina 29223.

^{b)}Permanent address: Institute for Electronic Science, Hokkaido University, Sapporo 060, Japan.

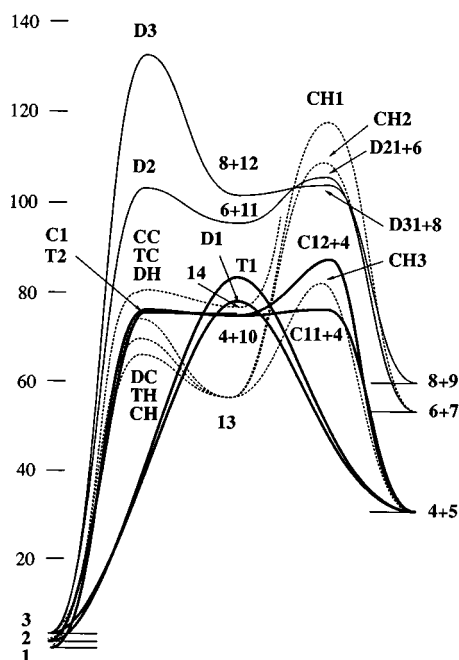


FIG. 1. Reaction paths on the ground PES of the dichloroethylene isomers, taken from Fig. 2 of Ref. 10. The potential energies (in kcal/mol) were calculated at the MP2/6-31G(*d,p*) level, using optimized geometries for HCl, H₂, and Cl₂ elimination. Bold lines are for processes initiated by HCl elimination, solid lines are for those initiated by H₂ or Cl₂ elimination, and dotted lines for those initiated by H or Cl migration. The numbers denote the following species: (1) *cis*-DCE, (2) *trans*-DCE, (3) 1,1-DCE, (4) HCl, (5) HCCCl, (6) H₂, (7) ClCCl, (8) Cl₂, (9) HCCH, (10) :C=CHCl, (11) :C=CCl₂, and (12) :CCH₂. Letters refer to transition states calculated in Ref. 10.

For *cis*-DCE, $\Delta H_0^0=53$ and 95 kcal/mol for the two pathways.¹⁰ The calculated enthalpies of formation of *trans*- and 1,1-DCE are, respectively, 0.1 and 0.6 kcal/mol greater than for *cis*-DCE.¹⁰

Although there have been no previous studies of the dynamics of H₂ elimination from DCE, there have been extensive studies of H₂ elimination from ethylene.¹¹ In a recent series of papers, Lee and co-workers examined the photodissociation of ethylene and its isotopomers at 193 nm.^{12–14} They found that (i) the quantum yields of H and H₂ are approximately equal; (ii) acetylene and vinylidene are produced in a ratio of 2:3; and (iii) the kinetic energy distribution of H₂ is peaked near 20 kcal/mol, indicating a concerted process with a substantial exit barrier.

Recently Morokuma and co-workers performed extensive *ab initio* calculations of the ground state potential energy surfaces of VCl,⁸ DCE,¹⁰ and ethylene.¹⁵ A diagram of all the pathways for molecular elimination from VCl is shown in Fig. 1 of paper I, while the corresponding diagram for DCE is shown in Fig. 1 of the present paper. Their calculations revealed three pathways that could lead to H₂ elimination. The lowest energy path for VCl, 1,1-DCE, and ethylene is 3CE via a late transition state, with barriers of 97.2, 101.4, and 93.8 kcal/mol, respectively. These barriers are considerably larger than those for 3CE of HCl (69.1, 76.6, and 76.1 kcal/mol for VCl, *cis*-DCE and *trans*-DCE).

The second mechanism is a hydrogen atom shift to form

a stable ethylidene intermediate (CH=CH₃, CCl=CH₃, and CCl=CH₂Cl), followed by H₂ elimination. The bridged transition state for the H shift has a barrier of 68.8 kcal/mol for VCl, 65.5 and 68.7 kcal/mol for *cis*- and *trans*-DCE, and 75.0 kcal/mol for ethylene. The elimination step has a subsequent barrier of 103.6 kcal/mol for VCl, 109.7 for DCE, and 109.5 for ethylene. (For VCl there is also a higher transition state at 115.3 kcal/mol.) The barriers for H migration are the lowest of any process on the ground PES, although the subsequent barriers to elimination of H₂ from the resulting radical are about 6 kcal/mol higher than for direct 3CE from VCl and DCE, and 14 kcal/mol higher than for direct 3CE from ethylene. It is important to note that direct 3CE from *cis*- and *trans*-DCE is not possible, while for 1,1-DCE hydrogen migration does not lead to H₂ elimination.

The third mechanism is direct four center elimination (4CE). True transition states were not found for this pathway, although second order tops converging to a migration path were located. Because the energies of these tops are very high (140.9, 151.9, and 125.3 kcal/mol for VCl, DCE, and ethylene), this pathway does not play a role in our experiments.

In this paper, we present a study of the UV photoelimination of H₂ from VCl and DCE. The fact that the absorption cross section of chloroethylenes are about three orders of magnitude larger than that of ethylene at 193 nm is a considerable advantage.³ Two types of information were obtained from these experiments. First, we measured the rotational populations of H₂(*v*"=0–4). Second, we used magic angle Doppler spectroscopy to characterize the translational energy distributions for several rotational states of H₂/VCl. Because of the large energy spacing of the rovibrational states of H₂ and the smaller amounts of energy available to the products, these measurements can be used to discriminate between possible reaction mechanisms.

II. EXPERIMENT

We will only give a brief summary of our apparatus here, since a detailed description has been presented elsewhere.¹⁶ Our apparatus is a pulsed molecular beam machine equipped with a standard Wiley–McLaren¹⁷ time-of-flight (TOF) mass spectrometer. A pump and probe technique was used in these experiments. An ArF (193 nm) excimer laser (Lambda Physik EMG150) was used to photodissociate the parent molecules, while the H₂ product was probed via 2+1 resonance-enhanced multiphoton ionization (REMPI) by a frequency-doubled excimer-pumped dye laser (Lambda Physik LPX200/LPD3002). The pump laser beam had a typical fluence of 40 mJ/cm² and was collimated with a 50 cm lens. The H₂⁺ ion was detected by a dual microchannel plate. The TOF tube was equipped with a pair of deflection plates that were biased to pass only H₂⁺ ions. The plates were grounded to allow H₂⁺ to pass through, and otherwise held at a potential difference of +200 V to shutter out the heavier ions. In the rotational population measurements the signal from the microchannel plate was averaged typically 100 times and recorded on a digital oscilloscope (LeCroy

9450A), while in the Doppler measurements the signal was averaged typically 30 times with a boxcar (Stanford Research) and recorded on a computer.

For measurements of the rotational population of H₂($v'' > 0$) the pump and probe laser beams were counter-propagated along an axis perpendicular to the molecular beam axis. The lasers and molecular beam intersected between the reflector and extractor plates in a plane normal to the TOF axis. The chloroethylene molecules were introduced into the reaction chamber via a pulsed valve (Newport BV-100V, 0.5 mm diam) fitted with a Teflon tip, located approximately 3 cm from the reaction zone. For H₂($v'' = 0$), the ArF laser was shut off and the dye laser served as both pump and probe. In the Doppler experiments the pump beam propagation vector, \mathbf{k}_d , was aligned at a 135° angle with respect to the probe beam propagation vector, \mathbf{k}_a . The pump beam was polarized with a pile of ten quartz plates set at the Brewster angle, oriented in such a way that the polarization vector of the pump beam, \mathbf{e}_d , formed a magic angle (54.74°) with \mathbf{k}_a . In addition, the polarization vector of the probe beam, \mathbf{e}_a , made a 45° angle with respect to the plane containing \mathbf{k}_a and \mathbf{e}_d . This combination of pump and probe alignment corresponds to the “double magic angle” geometry of Hall and Wu.¹⁸

The rotational population of H₂($X^1\Sigma_g^+, v'' = 0-4$) was measured using 2+1 REMPI with the E, F state as the resonant intermediate level.¹⁹ We recorded Q branches for all the ($v' = 0 \leftarrow v''$) bands. For $v'' = 1$ through $v'' = 4$, the probe wavelengths of 210–245 nm were generated by doubling the fundamental frequency of stilbene or Coumarin dyes, using a BBO(I) crystal for $\lambda \geq 220$ nm and a BBO(II) crystal otherwise. The fundamental frequency was not separated from the second harmonic until after the reaction zone, where the intensity of the doubled beam was monitored. We confirmed in test runs that this arrangement did not affect the results. The probe beam had a typical pulse energy of 0.5–1.0 mJ and was focused with a 15 cm focal length lens. The delay between the pump and probe pulses was set between 30 and 60 ns to maximize the signal to noise ratio.

For H₂($v'' = 0$), wavelengths between 201.65 and 206.46 nm were generated by first doubling the fundamental of Rhodamine 610 in a BBO(I) crystal, then mixing the doubled frequency with the fundamental in a BBO(II) crystal to produce sum frequency generation (SFG). As before, the beams were not separated until after they passed through the reaction zone. Again a test showed that the presence of the fundamental and second harmonic frequencies did not interfere with the experiment. The SFG beam had a typical energy of 40 μ J/pulse (measured after the reaction zone), and was focused with a 7 cm focal length lens.

The purity of the chloroethylenes was checked by NMR, confirming the manufacturer’s claims (VCl: >99.5% from Fluka; 1,1-DCE: 98%; *trans*-DCE: 99%; *cis*-DCE: 97%; all DCE’s obtained from Aldrich). The reagents were used without further purification. The neat sample gases were stored in a reservoir at ~ 180 Torr. The background pressure in the chamber was normally 10^{-6} Torr during a run, while the pressure in the reaction zone was estimated to be on the order of 10^{-3} Torr.

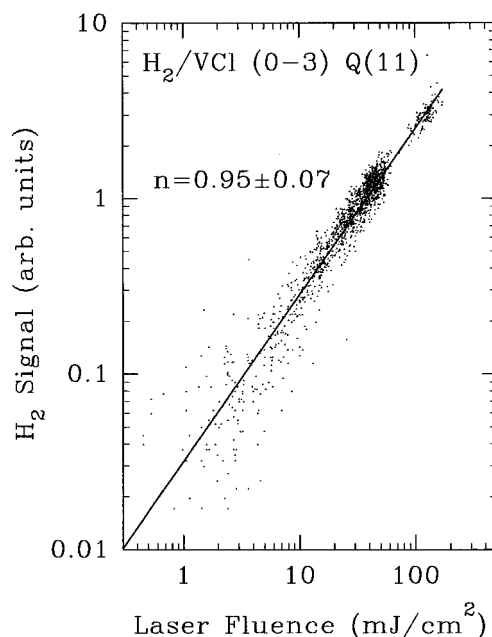


FIG. 2. Amplitude of the REMPI signal for the $Q(11)$ line of H₂($v'' = 3$)/VCl as a function of fluence of the photolysis laser. The solid line is a least squares fit of a power law, with the fitted value of the exponent listed in the plot.

In some experiments we measured the fragment concentration as a function of pump intensity. This was accomplished by placing an NH₃ absorption cell in the path of the pump laser beam. The laser intensity and REMPI signal were recorded on every shot as the NH₃ pressure was varied.

III. RESULTS

Five different types of experiments were performed. In the first two we studied the effects of varying the pump intensity and delay times. These diagnostics were needed to establish that the H₂ fragment is produced by single photon excitation. The main results of this study were obtained in the third and fourth sets of experiments, in which we measured the rotational populations and kinetic energy distributions of H₂. In a final experiment we searched for Cl₂, which is another possible photofragment of DCE.

A. Intensity dependence

The variation of the H₂ signal with pump laser intensity was measured for various rotational levels of H₂($v'' = 2$)/VCl and H₂($v'' = 2$)/1,1-DCE. Figure 2 shows a typical fluence dependence plot for the $Q(11)$ line of H₂($v'' = 3$)/VCl. The slopes of the log–log plots over three decades are all unity within one standard deviation, confirming that photodissociation is caused by a single pump photon.

B. Delay time

The previous experiment proves that only one pump photon is absorbed by the parent molecule. We also confirmed that the probe alone does not produce any H₂ signal for $v'' > 0$. (For $v'' = 0$ only one laser was used.) It is conceivable, however, that C₂H₃/VCl or C₂CH₂Cl/DCE produced by

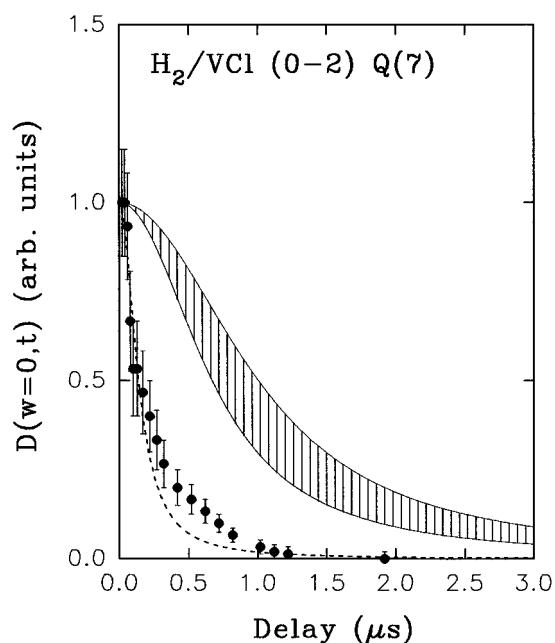


FIG. 3. Delay time study of the H₂($v''=2, J''=7$)/VCl signal. The abscissa is the delay between the pump and probe lasers, while the ordinate is the REMPI signal of H₂ at the center of the Doppler profile. The filled circles are experimental data with 1σ error bars. The shaded area was calculated assuming a $1+1'$ process, as described in the text. The dashed line was calculated assuming that H₂ flies out of the field of view immediately after absorbing one photon from the pump laser, with a kinetic energy equal to the mean value calculated from the magic angle Doppler profile.

the pump photon absorbs an additional photon from the probe beam to release H₂ (i.e., by a $1+1'$ process). This process is unlikely, however, since the probe wavelength for high v, J states is greater than 225 nm, while the extinction coefficient for simple olefinic hydrocarbons falls off very rapidly for $\lambda > 190$ nm.²⁰ A transient absorption measurement of vinyl for $\lambda < 190$ reported by Fahr and Laufer²¹ showed strong absorption only at 168.33 and 164.71 nm. The absorption coefficient of ethylene is of comparable magnitude at 170 nm and falls off 1000-fold at 190 nm.²⁰

The possibility that vinyl absorbs a probe photon and undergoes secondary decomposition can be tested by measuring how rapidly the H₂ signal decays with increasing delay between the two laser pulses. If H₂ were produced by only the pump laser, its decay would be determined by the rate at which H₂ flies out of the probe beam, whereas if it were produced by secondary photolysis its decay rate would be governed by fly-out of the much heavier vinyl or chlorovinyl radical.

A time delay study was performed on a set of rotational levels for H₂($v''=2$)/VCl. Figure 3 shows a typical result for the $Q(7)$ line of H₂($v''=2$)/VCl. The data points are the velocity aligned Doppler signal $D(w, t)$ measured at the central absorption frequency. The shaded area is the calculated signal assuming the speed distribution for the vinyl radical reported in paper I. (The width of this area is mainly due to uncertainty in the focal diameter of the laser beams, which was estimated from measurements of the beam profiles to lie between 0.5 and 1.0 mm.) The dashed line is the predicted

decay curve, based on the mean speed calculated from a magic angle Doppler spectrum of H₂ (see Sec. III D). It is clear from the figure that H₂ flies out of the reaction zone much faster than does the H₂CCH radical. At short delays the data overlap the simulated curve, showing that the H₂ fragment flies out of the field of view immediately after the photolysis pulse. The absence of signal at long delays places an upper bound of 10% for the $1+1'$ mechanism. (The discrepancy with the calculation at intermediate times is most likely due to the simplification of using the mean H₂ speed in the simulation. This approximation was necessary because the complete speed distribution function of H₂ could not be extracted quantitatively from the Doppler profile.) Very similar results were obtained for the $Q(11)$ and $Q(13)$ lines of H₂($v''=2$).

C. Rotational populations

The rotational populations of H₂ in different vibrational states v'' were extracted from the Q branches of the $2+1$ REMPI spectra of the $E, F \leftarrow X(v' = 0 \leftarrow v'')$ transition, using the expression,²²

$$I(v', J'; v'', J'') = CP(v'', J'')g_I(J'') \times q(v', v'')S(J', J'')/(2J'' + 1), \quad (3)$$

where $I(v', J'; v'', J'')$ is the signal intensity corresponding to the $E, F(v', J') \leftarrow X(v'', J'')$ transition, C is an apparatus constant, $P(v'', J'')$ is the population of H₂(v'', J''), $g_I(J'')$ is the nuclear spin degeneracy (1 for odd J'' and 3 for even J''), $q(v', v'')$ is the Franck–Condon factor, and $S(J', J'')$ is the rotational line strength.

From the observed peak heights we can determine the relative rotational state populations within a single vibrational level, provided that the line strength factor is known. If the upper state of H₂ were unperturbed, this quantity would be simply the Hönl–London factor. But in fact the inner well E is accidentally perturbed by the outer well F . The effective rotational line strengths have been determined experimentally and theoretically by Zare and Huo^{23,24} for the transitions ($v' = 0 \leftarrow v'' = 0, 1, 2$). The line strengths are close to, but differ from, unity.

We have recorded the rotational spectra for H₂($v''=0-4$)/VCl, H₂($v''=0-4$)/1,1-DCE, H₂($v''=2-4$)/*cis*-DCE, and H₂($v''=2$)/*trans*-DCE. The resulting populations of H₂($v''=0-2$)/VCl and H₂($v''=0-2$)/1,1-DCE are shown in Figs. 4 and 5 in the form of bar graphs and in Figs. 6 and 7 as “Boltzmann plots,” where the correction for even and odd nuclear spin statistics has been included.²⁵ The highest internal energy observed was 75.4 kcal/mol, corresponding to $J''=17, v''=3$. As shown in the figures, all the rotational state distributions have linear Boltzmann plots, with temperatures around 3000 K.

In Fig. 8 we compare the rotational distributions of H₂($v''=2$) produced from the three DCE isomers. It is seen that the three isomers have different rotational temperatures, in the order $1,1 < cis < trans$. This is in contrast with the HCl fragment, which has nearly the same rotational state distributions for all three isomers.

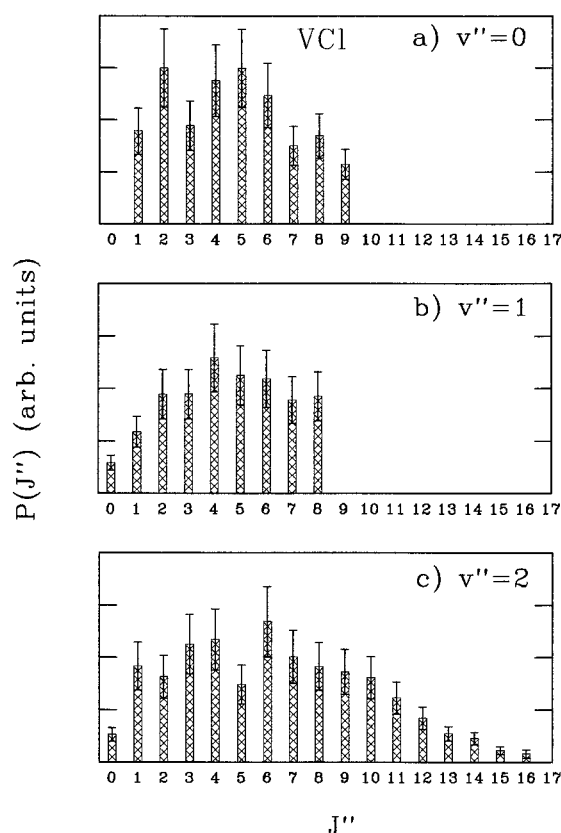


FIG. 4. Rotational population of H₂($v''=0, 1$, and 2) produced from VCl, calculated from the peak heights in the REMPI spectrum using empirical line strength factors (Ref. 23) and corrected for nuclear degeneracy. The ordinate is in arbitrary units, and the scales of the different panels do *not* indicate relative yields. Error bars are single standard deviations obtained from two or more scans of the spectrum.

In Figs. 9 and 10 are plotted the rotational state distributions for H₂($v''=3$ and 4) obtained from VCl, *cis*-DCE, and 1,1-DCE, where we have assumed that the unknown rotational line strengths for $v''=3$ and 4 are independent of J'' . Since the true line strengths are probably not constant, the rotational temperatures in these plots are not reliable. The comparison of the relative H₂ populations produced from different parent molecules is nevertheless meaningful, and the Boltzmann plots do reveal trends in the data. In particular, it is seen that H₂/*cis*-DCE is hotter than H₂/1,1-DCE, while H₂/1,1-DCE and H₂/VCl have approximately the same rotational temperatures, continuing the pattern found for lower vibrational states.

The relative quantum yields of H₂ produced from the DCE isomers were measured for $v''=2$, $J''=3$. These yields were found to be in the ratio 1.0:0.18:0.13 for 1,1-, *trans*-, and *cis*-DCE, respectively. Summing over all rotational levels (and extrapolating to large J''), the relative quantum yields for $v''=2$ are 1.0:0.32:0.18. The yields of H₂/VCl and H₂/1,1-DCE were found to be comparable, with the 1,1-yield tending to be 10%–20% larger.

D. Maximum and mean translational energy

Doppler profiles were recorded for the $v''=2$, $J''=3, 5, 7, 9$, and 11 levels of H₂/VCl. A typical result is shown in Fig.

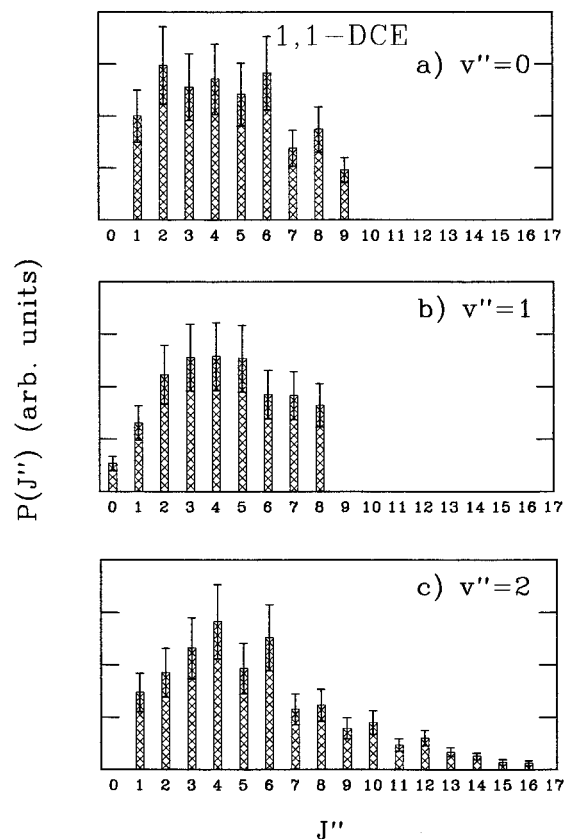


FIG. 5. Same as Fig. 4, only for H₂/1,1-DCE.

11. Unlike the case for Cl detachment in paper I, the signal to noise ratio was not high enough to extract quantitative speed distribution functions. Nevertheless, we can obtain from the data the maximum speed and the first few moments of the distribution function. In the Appendix we show that, in the absence of $\mathbf{v} \cdot \mathbf{J}$ correlation,²⁶ these moments can be extracted as a simple quadrature,

$$\langle v^n \rangle = (n+1) \frac{\int_0^\infty v^n D(v) dv}{\int_0^\infty D(v) dv}. \quad (4)$$

The results are displayed in Fig. 12.

E. Cl₂ elimination

Using the same experimental conditions as in the H₂ elimination study, we searched unsuccessfully for Cl₂/1,1-DCE and Cl₂/*cis*-DCE, using 2+1 REMPI with the spectroscopically allowed $V' 2^1\Pi_g$ state as the intermediate resonance state.^{27,28} To calibrate the sensitivity of our measurement, we first detected the Cl₂⁺ REMPI signal from a known Cl₂ gas sample. Our failure to observe Cl₂ places a rough upper bound on its quantum yield of 0.1%.

IV. DISCUSSION

The results of Secs. III A and III B demonstrate that H₂ is produced by a single photon of the pump laser. Under our experimental conditions, rotational and translational relax-

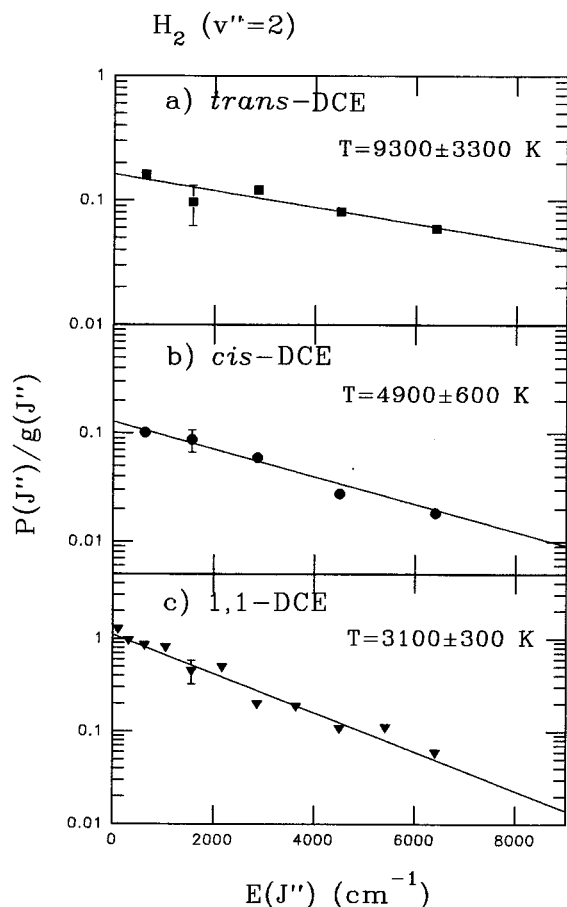


FIG. 8. Same as Fig. 6, only for H₂($v''=2$) produced by photodissociating *trans*-, *cis*-, and 1,1-DCE. (The prior distributions are not shown in this figure.) Notice that the data in panel (c) are identical to those in Fig. 7(c), redrawn to scale. In this figure only, the ordinates indicate relative yields from different parent molecules.

by 3CE is $J''=12$, while we observed $J''=17$. For $v''=4$, the highest J'' that can be populated by 3CE is 9, while we observed $J''=13$. The discrepancy would be even greater if the relative translational energy were taken into account.

Similar considerations apply to DCE. Magic angle Doppler profiles were measured for $J''=3, 5, 7, 9$, and 11 of H₂($v''=2$)/1,1-DCE. Although the signal/noise ratio was insufficient for quantitative analysis, from the widths of the Doppler profiles it is clear that the internal plus recoil energy of H₂ exceeds the available energy for a 3CE mechanism. The very high rotational levels observed for $v''=3$ and 4 (Figs. 9 and 10) are further proof of a 4CE mechanism. For *cis*- and *trans*-DCE the signal levels were too low to record magic angle Doppler spectra. Nevertheless we observed very high rotational levels for H₂/*cis*-DCE which are energetically forbidden by 3CE.

While the data clearly establish the existence of a four center mechanism at high J , the evidence here for a 3CE path is not as conclusive. None of the Boltzmann plots exhibit a break at the 3CE energy limit. There is a minimum at $J''=5$ for both H₂($v''=2$)/VCl and H₂($v''=2$)/1,1-DCE, which was also observed by Stolow *et al.*¹³ for H₂($v''=2$)/C₂H₄. For ethylene, Balko *et al.*¹² demonstrated

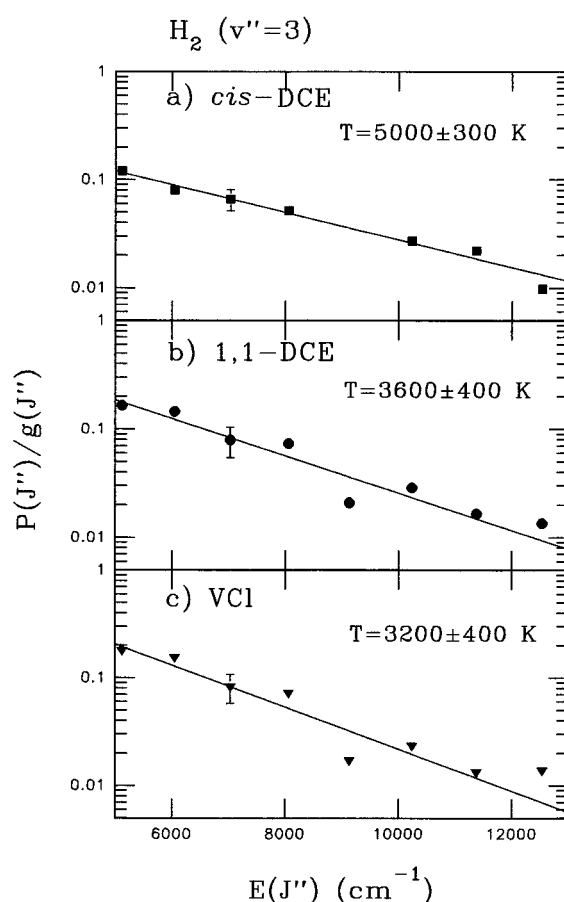


FIG. 9. Same as Fig. 6, only for H₂($v''=3$) produced from *cis*-DCE, 1,1-DCE, and VCl. Notice that while the trends are reliable, the rotational temperatures are inaccurate because of the lack of empirical line strength factors for H₂($v''=3$). The data points correspond to rotational levels $J''=10-17$.

by deuterium labeling that the total quantum yield for the three-center path is 1.5 times that for the four-center path. It was suggested,⁴ though not proven, that the minimum at $J''=5$ is indicative of 3CE dominating at low J and 4CE at high J . The striking similarity between the rotational populations of H₂ for all three molecules suggests a common mechanism.

For ethylene, Stolow *et al.*⁴ fit the rotational Boltzmann plots with biexponential functions, with the low temperature component assigned to 3CE and the high temperature component assigned to 4CE. The branching between the two paths was fixed by arbitrarily assigning a vibrational temperature for the 3CE path half of that of the 4CE path. Also, the 3CE rotational temperatures for $v''=0$ and 1 were assumed to equal the values deduced from the isotopic experiments. For VCl and 1,1-DCE this independent information is unavailable. Treating the two rotational temperatures and the 3CE/4CE branching ratio of H₂($v''=2$) as independent least squares parameters, we obtain 3CE contributions of 8% and 55% for VCl and 1,1-DCE, as compared with the assumed value of 32% for ethylene. The fitted rotational temperatures for all three molecules are similar. While the branching fractions are quite different, in the absence of isotopic data it is reasonable to conclude that 3CE contributes to the photodis-

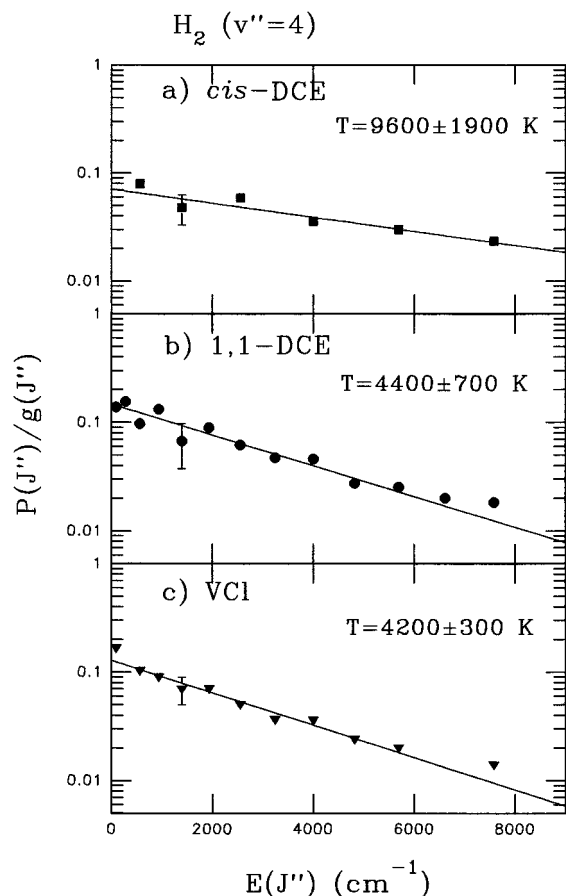


FIG. 10. Same as Fig. 9, only for H₂(v''=4) and J''=0–13.

sociation mechanisms of VCl and 1,1-DCE at low J . Further evidence of a three-center mechanism is seen in the larger quantum yields of H₂(v''=2) produced from VCl and 1,1-DCE, as compared with *cis*- and *trans*-DCE. Since for the

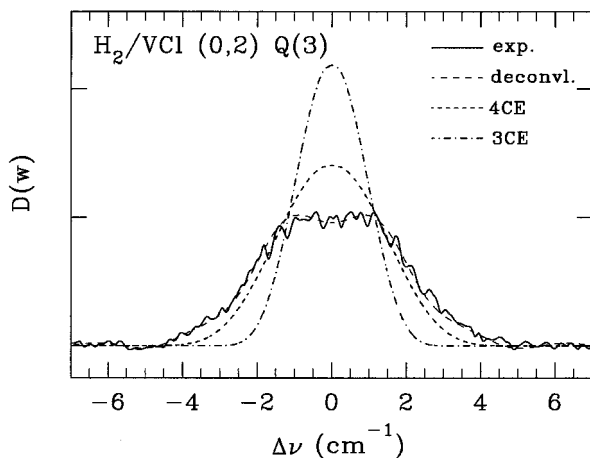


FIG. 11. Doppler profile for the $Q(3)$ line of H₂(v''=2)/VCl. Superimposed on the data is a smooth curve representing a ten term Hermite polynomial fit of the data, which was deconvoluted to correct for the bandwidth of the laser and thermal motion of the parent molecules. The dashed line is calculated assuming a prior translational energy distribution with the available energy from four-center elimination, while the dot-dashed curve is the prior calculation for three-center elimination. All curves are normalized to unit area.

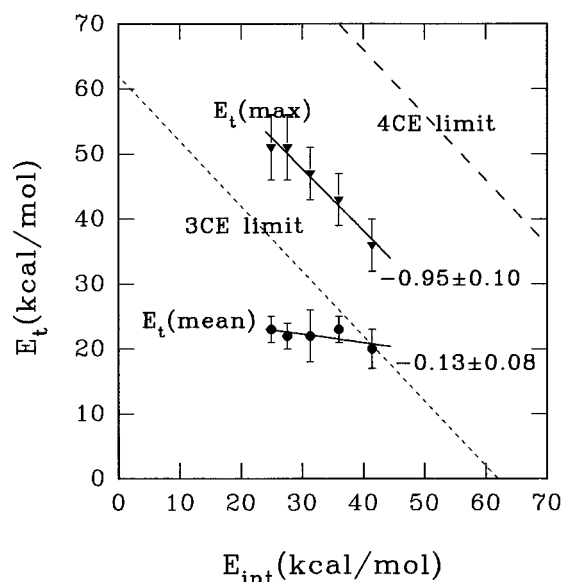


FIG. 12. Mean and maximum recoil energies of H₂(v''=2)/VCl as functions of internal energy of the H₂ fragment. Points are for $J''=3, 5, 7, 9,$ and 11 . Solid lines are least squares fits with the indicated slopes. The dashed lines are the maximum available energy for three- and four-center elimination. These lines include an estimated 5 kcal/mol added to account for internal energy of the parent molecule.

latter two compounds a three-center mechanism is impossible (unless both H and Cl migrate), a smaller quantum yield of H₂ is expected.

Additional information about the disposal of energy may be learned from the mean and maximum recoil energies of H₂(v''=2)/VCl plotted in Fig. 12. The weak dependence of the mean recoil energy on E_{int} is a measure of the increasing contribution from 4CE at high J (e.g., a higher rotational “temperature” for 4CE as compared with 3CE). The similarity between the slopes of this plot for VCl (-0.13 ± 0.08) and C₂H₄ (-0.213 , Fig. 8 of Ref. 14) is a further indication of the similarity of the H₂ elimination mechanisms for these two molecules.

The observation that the maximum recoil energy lies between, and is parallel to, the 3CE and 4CE limits indicates that a fixed amount of energy (≈ 28 kcal/mol) is deposited into the acetylene fragment. This energy must be sharply peaked in order to produce the observed cutoff in the H₂ Doppler profiles. Excitation of C₂H₂ could be caused by a Franck–Condon effect resulting from the fact that the C–C bond in the transition state is compressed by ~ 0.1 Å, as compared with the equilibrium distance in free chloroacetylene.^{8,10} A rough calculation gives a value of 9.7 kcal/mol for the C–C stretch assuming a bond compression of 0.087 Å. Excitation of other vibrational modes as well as an additional impulse from the departing H₂ are possible.

B. Reaction path

In the previous section we demonstrated that 4CE is the dominant mechanism for H₂ elimination from VCl and DCE at high v and J , and that 3CE is likely to contribute to the mechanism at lower J for VCl and 1,1-DCE. We inquire next into the microscopic details of the reaction mechanism. Di-

rect 4CE is Woodward–Hoffman forbidden, and indeed Morokuma *et al.*^{8,10} failed to find a true transition state for this path. The alternative for four-center elimination is a hydrogen atom migration in VCl, *cis*-DCE, and *trans*-DCE and a Cl shift in 1-1 DCE to produce a chloro-ethylidene intermediate (structure 13 in Fig. 1). The barriers for atom migration are substantially lower than for direct 3CE, making this the most likely first step. The three-center mechanism can compete with 4CE since the secondary barrier for elimination of H₂ from the radical intermediate is slightly higher than the barrier for 3CE. If sufficient energy is unavailable along the 4CE reaction coordinate, the molecule may undergo remigration and eventually react by 3CE. Molecules which do react by 4CE apparently retain memory of their initial conditions, since the rotational temperatures for H₂ produced from the three DCE isomers (Figs. 8–10) are quite different.

In the previous literature there has been considerable discussion regarding partitioning of the available energy among the fragments. For HCl elimination, Berry introduced the concept of “localized energy,” meaning that only the energy above the exit barrier is distributed statistically among the products, whereas the barrier energy is released impulsively into internal energy of HCl and relative translational energy of the fragments.²⁹ This idea was refined by Zamir and Levine^{30,31} and Umemoto *et al.*³² who also concluded that the barrier energy is released impulsively. Nonstatistical energy release is expected also for H₂ elimination, for which Morokuma *et al.* calculated substantial exit barriers for the migration mechanism (Fig. 1).^{8,10} For example, in the case of H₂/VCl the reverse barrier is calculated to be 57 kcal/mol for the migration channel, as compared with 6–7 kcal/mol for 3CE.

The Doppler profile for H₂(*v*''=2, *J*''=3)/VCl is compared in Fig. 11 with the statistical predictions for 3CE and 4CE, ignoring **v**·**J** correlation. The experimental profile is noticeably broader than either model calculation. If we assume that **J** is perpendicular to **v** (*g*₂= $\frac{1}{2}$), the data are still markedly different from the 3CE profile, but are only slightly broader than the 4CE result. Additional experiments with single photon detection of H₂ would be helpful to determine the amount of rotational correlation.

Departure from statistical behavior is apparent in the rotational temperatures of H₂/VCl and H₂/1,1-DCE, which increase slightly with vibrational energy (Figs. 6 and 7). The fact that the rotational populations have Boltzmann-type functions does not imply statistical behavior.³³ The 4CE prior distribution is in good agreement with the data for *v*''=2, but gets progressively hotter than experiment at lower *v*''. In comparison, the 3CE prior distribution agrees well with the data for *v*''=0, but is very much colder at *v*''=2.

C. Relative quantum yields

In Table I are listed the branching fractions for all atomic and diatomic fragments of the DCE isomers. These numbers are based on the [Cl]/[HCl] ratios measured by Umemoto *et al.*³² for *cis*- and *trans*-DCE, the yields of H, Cl, and HCl from *cis*- and *trans*-DCE relative to the yields from 1,1-DCE measured by He *et al.*,⁵ the ratio of [Cl]/[H] for 1,1-DCE

TABLE I. Relative product yields for the photodissociation of DCE.

Parent molecule	Percentage yield of fragment ^a				
	H ^b	Cl(² P _{3/2}) ^b	Cl(² P _{1/2}) ^b	HCl ^{b,c}	H ₂ (<i>v</i> ''=2)
<i>cis</i> -DCE	3.3	65.3	9.8	20.5 ^d	0.9 ^e
<i>trans</i> -DCE	4.2	54.2	8.1 ^f	32.0 ^d	1.5 ^e
1,1-DCE	12.7 ^f	49.3	16.0 ^f	17.0	5.0 ^g

^aThe precision of the entries is limited by the published uncertainties, and is generally no worse than ±20%.

^bRelative yields taken from Ref. 5.

^cNormalization of yields of different vibrational levels calculated from Refs. 29 and 39.

^dBranching ratios of [HCl]/[Cl] taken from Ref. 32.

^eBased on the relative yields of H₂(*v*''=2) in the present paper, summed over all rotational levels.

^fBranching ratios of [H]/[Cl] and [Cl(²P_{1/2})]/[Cl(²P_{3/2})] taken from Ref. 1.

^gAdapted from Ref. 7.

measured by Mo *et al.*,¹ the quantum yield of H₂/VCl measured by Ausloos *et al.* at 147 nm,⁷ and the present measurements of the relative yields of H₂(*v*''=2) for VCl and DCE. Although the various data sets are consistent within their experimental errors, small uncertainties in some entries can lead to large errors for the minor products. To deal with this difficulty we preserved the relative yields of H₂ for different DCE isomers, as well as the relative yields of H, and the Cl(²P_{1/2})/Cl(²P_{3/2}) branching ratio for *cis*-DCE, while allowing the absolute values for Cl to vary within their experimental errors.

We see in this table that the main fragment is Cl, followed by HCl, H, and H₂. We already pointed out that the much smaller yields of H₂ from *cis*- and *trans*-DCE as compared with 1,1-DCE and VCl is likely to be due to the absence of a three-center path for the former. Another interesting result is that the relative quantum yields of H, H₂, and HCl are all 30%–60% larger for *trans*-DCE than for *cis*-DCE. For the H atom fragment we might expect the yields to be equal since the C–H bonds are nearly identical for the two isomers on the ground PES. A possible explanation of the different yields is that *cis*-DCE undergoes faster Cl detachment on the upper PES, thereby reducing all the quantum yields on the ground PES. If reaction on the excited PES did not occur, we would expect the relative yields of Cl and H to be equal for *cis*- and *trans*-DCE, since they depend only on the RRKM rate constants for atom detachment. The fact that we observe a larger Cl/H ratio for *cis*-DCE is indicative of a greater rate of Cl detachment on the upper surface. For molecular elimination there is the additional factor that the transition states for the two isomers on the lower PES need not be identical. In the case of HCl elimination, the rotational populations are nearly identical for all three isomers, showing that the transition states are in fact similar. Consequently, for HCl we attribute the different quantum yields to Cl detachment on the upper surface. For H₂ the rotational populations vary for the different isomers, indicating that effects on both surfaces may be important. Visual inspection of the translational energy distributions, *p*(*E_t*), for Cl/*cis*-DCE and Cl/*trans*-DCE in paper I and in the work of Suzuki *et al.*³⁴ does suggest a greater reactivity of *cis*-DCE on the upper surface. Unfortunately, the partitioning of *p*(*E_t*) into compo-

- ¹⁰J.-F. Riehl, D. G. Musaev, and K. Morokuma, *J. Chem. Phys.* **101**, 5942 (1994).
- ¹¹For a review, see G. J. Collin, *Adv. Photochem.* **14**, 136 (1988).
- ¹²B. A. Balko, J. Zhang, and Y. T. Lee, *J. Chem. Phys.* **97**, 15 (1992).
- ¹³A. Stolow, B. A. Balko, E. F. Cromwell, J. Zhang, and Y. T. Lee, *J. Photochem. Photobiol. A: Chem.* **62**, 285 (1992).
- ¹⁴E. F. Cromwell, A. Stolow, M. J. J. Vrakking, and Y. T. Lee, *J. Chem. Phys.* **97**, 4029 (1992).
- ¹⁵J. H. Jensen, K. Morokuma, and M. S. Gordon, *J. Chem. Phys.* **100**, 1981 (1994).
- ¹⁶Y. Xie, P. T. A. Reilly, S. Chilukuri, and R. J. Gordon, *J. Chem. Phys.* **95**, 854 (1991).
- ¹⁷W. C. Wiley and I. H. McLaren, *Rev. Sci. Instrum.* **26**, 1150 (1955).
- ¹⁸G. E. Hall and M. Wu, *J. Phys. Chem.* **97**, 10 911 (1993).
- ¹⁹G. Herzberg, *Molecular Spectra and Molecular Structure. IV. Constants of Diatomic Molecules* (Van Nostrand-Reinhold, New York, 1979).
- ²⁰L. C. Jones, Jr. and L. W. Taylor, *Anal. Chem.* **27**, 228 (1955).
- ²¹A. Fahr and A. Laufer, *J. Phys. Chem.* **92**, 7229 (1988); A. Laufer (private communication).
- ²²G. Herzberg, *Molecular Spectra and Molecular Structure. I. Spectra of Diatomic Molecules* (Van Nostrand, Princeton, 1950), p. 126.
- ²³K.-D. Rinnen, M. A. Buntine, D. A. V. Kliner, R. N. Zare, and W. M. Huo, *J. Chem. Phys.* **95**, 214 (1991).
- ²⁴W. M. Huo, K.-D. Rinnen, and R. N. Zare, *J. Chem. Phys.* **95**, 205 (1991).
- ²⁵W. S. Struve, *Fundamentals of Molecular Spectroscopy* (Wiley, New York, 1989), p. 149.
- ²⁶R. N. Dixon, *J. Chem. Phys.* **85**, 1866 (1986).
- ²⁷L. Li, R. J. Lipert, H. Park, W. A. Chupka, and S. D. Colson, *J. Chem. Phys.* **88**, 4608 (1988).
- ²⁸B. G. Koenders S. M. Koeckhoven, G. J. Kuik, K. E. Drabe, and C. A. de Lange, *J. Chem. Phys.* **91**, 6042 (1989).
- ²⁹M. J. Berry, *J. Chem. Phys.* **61**, 3114 (1974).
- ³⁰R. D. Levine and J. L. Kinsey, in *Atom-Molecule Collision Theory: A Guide for the Experimentalist*, edited by R. B. Bernstein (Plenum, New York, 1979), pp. 693–750.
- ³¹E. Zamir and R. D. Levine, *J. Chem. Phys.* **52**, 253 (1980).
- ³²M. Umemoto, K. Seki, H. Shinohara, U. Nagashima, N. Nishi, M. Kinoshita, and R. Shimada, *J. Chem. Phys.* **83**, 1657 (1988).
- ³³R. Schinke, *Photodissociation Dynamics: Spectroscopy and Fragmentation of Small Polyatomic Molecules* (Cambridge, New York, 1993).
- ³⁴T. Suzuki, K. Tonokura, L. S. Bontuyan, and N. Hashimoto, *J. Phys. Chem.* **98**, 13 447 (1994).
- ³⁵J. D. Ewbank, J. Y. Luo, J. T. English, R. Liu, W. L. Faust, and L. Schäfer, *J. Phys. Chem.* **97**, 8745 (1993).
- ³⁶M. G. Moss, M. D. Ensminger, and J. D. McDonald, *J. Chem. Phys.* **74**, 6631 (1981).
- ³⁷M. P. Docker, *J. Chem. Phys.* **135**, 405 (1989).
- ³⁸A. Orr-Ewing and R. N. Zare, in *Chemical Dynamics and Kinetics of Small Radicals*, edited by A. Wagner and K. Liu (World Scientific, Singapore, 1995).
- ³⁹D. J. Donaldson and S. R. Leone, *J. Chem. Phys. Lett.* **132**, 240 (1986).